Published in final edited form as:
Exp Cell Res. 2011 May 1; 317(8): 1226–1237. doi:10.1016/j.yexcr.2011.01.020.

Cardiac-Specific NRAP Overexpression Causes Right Ventricular Dysfunction in Mice

Shajia Lu[1,*], **Garland L. Crawford**[1,*], **Justin Dore**[1], **Stasia A. Anderson**[2], **Daryl DesPres**[3], and **Robert Horowits**[1]

[1]National Institute of Arthritis and Musculoskeletal and Skin Diseases National Institutes of Health, Department of Health and Human Services Bethesda, MD 20892

[2]National Heart Lung and Blood Institute National Institutes of Health, Department of Health and Human Services Bethesda, MD 20892

[3]National Institute of Neurological Disorders and Stroke and Mouse Imaging Facility National Institutes of Health, Department of Health and Human Services Bethesda, MD 20892

Abstract

The muscle-specific protein NRAP is concentrated at cardiac intercalated disks, plays a role in myofibril assembly, and is upregulated early in mouse models of dilated cardiomyopathy. Using a tet-off system, we developed novel transgenic lines exhibiting cardiac-specific NRAP overexpression ~ 2.5 times greater than normal. At 40-50 weeks, NRAP overexpression resulted in dilation and decreased ejection fraction in the right ventricle, with little effect on the left ventricle. Expression of transcripts encoding brain natriuretic peptide and skeletal α-actin was increased by cardiac-specific NRAP overexpression, indicative of a cardiomyopathic response. NRAP overexpression did not alter the levels or organization of N-cadherin and connexin-43. The results show that chronic NRAP overexpression in the mouse leads to right ventricular cardiomyopathy by 10 months, but that the early NRAP upregulation previously observed in some mouse models of dilated cardiomyopathy is unlikely to account for the remodeling of intercalated disks and left ventricular dysfunction observed in those cases.

Keywords

NRAP; cardiomyopathy; heart; intercalated disk; transgenic; tetracycline-controlled transactivator

INTRODUCTION

The cardiac intercalated disk is a complex structure found at the longitudinal ends of cardiomyocytes [1]. The adherens junction region of the intercalated disks is where myofibrils terminate and link to complexes of membrane-associated proteins inside the cardiomyocyte, and where cardiomyocytes are mechanically coupled to each other through homophilic interaction of N-cadherin molecules embedded in the membranes of adjacent

Address for Correspondence: Dr. Robert Horowits Building 50, Room 1154 MSC 8024 National Institutes of Health Bethesda, MD 20892-8024 Telephone: 301-435-8371 horowits@helix.nih.gov.
*These authors contributed equally to this work.

cells. These connections allow mechanical force generated by the myofibrils to be transmitted to the membrane and neighboring cells. Intercalated disks are also responsible for electrical coupling between neighboring cardiomyocytes via gap junctions formed by connexin-43.

NRAP is a striated muscle-specific protein that is concentrated at intercalated disks in cardiac muscle and at myotendinous junctions in skeletal muscle [2]. Ultrastructural studies showed that NRAP is located in the terminal actin bundles that link the ends of the myofibrils to the membranes [3,4]. NRAP is a multidomain scaffolding protein with many potential binding partners [5-7]. Its N-terminal LIM domain can bind talin and α-actinin; its single nebulin repeats can bind α-actinin, actin, muscle LIM protein (MLP) and Krp1; and its nebulin-related super repeats can bind actin, vinculin, filamin and Krp1. On the basis of its domain organization, subcellular localization, and multiple binding partners, we hypothesized that NRAP may serve a mechanical role, linking the terminal actin filaments of myofibrils to the specific proteins concentrated in these junctional regions [7]. This model was further supported by biochemical copurification of NRAP with cardiac intercalated disks, as well as with isolated, detergent washed myofibrils, demonstrating NRAP's tight association with both myofibril ends and the membrane-associated structures to which they attach [4]. Subsequent experiments have implicated NRAP as an obligatory molecular scaffold in the first steps of myofibril assembly [8-10].

Changes in the expression of NRAP and other components of cardiac intercalated disks have been observed in dilated cardiomyopathy (DCM) [6,11,12]. DCM is a prevalent disease of the heart characterized by dilated and poorly functioning ventricles [13]. Greater than 20% of cases appear to have a genetic basis, and a diverse group of genes have been identified as dominant loci for the disease [14]. Several of these genes encode cytoskeletal proteins, leading to the suggestion that compromised force transmission is one primary cause of DCM [14,15]. The DCM-causing genes at many other loci remain unidentified [14].

Previous studies showed that NRAP protein levels are increased in two genetic mouse models of DCM [6]. One of these is the muscle LIM protein (MLP) knockout mouse [16], while the second is a tropomodulin-overexpressing transgenic (TOT) mouse [17]. MLP protein is also decreased in the TOT mouse [6]. In both mouse models, NRAP upregulation occurs soon after birth, preceding other molecular and morphologic changes associated with the cardiomyopathy. MLP directly binds NRAP in vitro [6], and MLP mutations associated with human cardiomyopathy have been shown to lead to decreased MLP binding to NRAP and α-actinin [18]. These findings implicate increased NRAP expression in the pathogenesis of cardiomyopathy.

Here we use the cardiac-specific tet-off transgenic mouse system [19] to directly test the effects of NRAP overexpression on cardiac structure and function. We found that the NRAP-overexpressing transgenic animals exhibited right ventricular dilation and dysfunction, with little effect on the left ventricle. The results demonstrate that the excess NRAP expression observed in the MLP knockout mouse and the TOT mouse is unlikely to account for the development of left ventricular DCM in those systems.

MATERIALS AND METHODS

Transgenic Animals

A transgene was designed to express full length mouse cardiac NRAP under control of the tetracycline-controlled transactivator protein (tTA) (Figure 1A). The coding region of the complete mouse cardiac NRAP cDNA was cloned into the pTRE2hyg2-Myc plasmid (Clontech Laboratories, Mountain View, CA) as previously described [8]. The final

construct matched the exons embedded in the mouse genomic DNA sequence (Genbank GenInfo Identifier number 20890983). The 8375 bp transgene encoding myc-NRAP was excised by double digestion with HpaI and PvuI. Transgenic mice were produced from this construct by standard pronuclear microinjection of fertilized FVB mouse eggs and screened by Southern blot under a contract agreement with the Laboratory Animal Sciences Program of the National Cancer Institute (Frederick, MD).

Mice expressing tTA specifically in the heart under control of the rat α-myosin heavy chain promoter [19] were rederived from frozen embryos obtained from the Jackson Laboratory (Bar Harbor, ME; strain FVB/N-Tg(MHCAtTA)6Smbf/J). In our hands the resulting male animals were infertile when mated with wild type or myc-NRAP transgenic females. Therefore all matings with this strain were performed using only the female mice.

The myc-NRAP and tTA transgenic strains were propagated by mating with wild type FVB mice. The hemizygous myc-NRAP transgenic males were mated with tTA transgenic females to produce double transgenic, single transgenic, and wild type animals for experiments. All pups were weaned at 3 weeks after birth. In pilot experiments, some animals were exposed to doxycycline (dox) to suppress transgene expression; mating pairs were fed dox diet pellets containing 400 mg dox/kg (Bio-Serv, Frenchtown, NJ). At weaning all pups were placed on a normal diet without dox.

All animals were assayed for the presence of the myc-NRAP and tTA transgenes by PCR analysis of genomic DNA. Genomic DNA was isolated from tail biopsies using the iPrep ChargeSwitch gDNA Tissue Kit (Invitrogen Corporation, Carlsbad, CA), and PCR was performed using the Advantage 2 PCR Kit (Clontech, Mountain View, CA) and the primers listed in table 1. The amplification protocol was 1 cycle at 95 °C for 1 minute; 30 cycles at 95 °C for 30 seconds, then 68 °C for 1 minute; and then 1 cycle at 68 °C for 1 minute. PCR products were visualized by agarose gel electrophoresis.

Protein Isolation and Immunoblotting

Mouse tissues were dissected and stored at −80 °C until use. Samples were prepared for immunoblot analysis [2], and equal amounts of protein were separated by gel electrophoresis, blotted to PVDF, and probed with antibodies as previously described [9]. Primary polyclonal antibodies against NRAP [2] and nonmuscle myosin heavy chain IIB (NMHC IIB) (Covance, Emeryville, CA) were diluted 1:2000, and antibody against connexin-43 (Sigma-Aldrich, St. Louis, MO) was diluted 1:5000. Monoclonal antibodies against c-Myc (Clontech, clone 9E10), N-cadherin (Research Diagnostics, Flanders, NJ, RDI-NCADHERabm), and GAPDH (Abcam, Cambridge, MA, clone 6c5) were diluted 1:200, 1:1000, and 1:5000 respectively. Stabilized goat anti-rabbit and anti-mouse HRP conjugated secondary antibodies (Pierce, Rockford, IL) were used at 1:2000 to 1:5000 dilutions. Protein levels were quantitated by densitometric analysis and normalized to GAPDH in the same samples.

RNA Isolation and Real-Time PCR

Total RNA was purified from mouse tissues [20], first-strand cDNA synthesized and gene expression quantitated by real-time PCR [9] as previously described. PCR primers are indicated in Table 1. The amplification protocol was 1 cycle at 95 °C for 10 minutes; 40 cycles at 95 °C for 30 seconds, then 60 °C for 1 minute, then 72 °C for 30 seconds. In simultaneously run reactions, 18s rRNA was amplified using QuantumRNA 18s Universal Internal Standard primers (Ambion). Gene expression was normalized to 18s mRNA levels in the same sample, and the normalized values were expressed as a fraction of the value in wild type controls.

Light Microscopy

Mice were euthanized by CO_2 inhalation. Hearts were dissected and immersed for 20 minutes in relaxation buffer (80 mM potassium acetate, 10 mM potassium phosphate, 5mM EGTA, pH 7.2-7.4), rinsed in PBS, and fixed in PBS containing 4% paraformaldehyde for 1 hour. The fixed hearts were cryoprotected in PBS containing 30% sucrose at 4°C overnight, then frozen for sectioning. Transverse frozen sections were cut 10 μm thick, and sections at 100-150 μm intervals were stained with hematoxylin and eosin (H&E) (Histoserve, Inc. Germantown, MD). Unstained frozen sections were stored at −80°C and used for antibody staining.

Low magnification images of H&E stained transverse heart sections were captured using an Olympus SZX9 dissecting microscope with a 1X objective and a Spot Insight 2 Megapixel CCD camera. Ventricular wall thicknesses and chamber diameters were averaged from measurements taken from five sections adjacent to the largest transverse diameter of each heart.

For immunofluorescence, frozen sections were thawed, rinsed in PBS for 5 minutes and then immersed in methanol at −20 °C for 20 minutes. Slides were quickly rinsed in PBS, then washed in 0.1% Nonidet P-40 in PBS for 3 minutes at room temperature. Slides were processed for immunofluorescence using the Vector M.O.M. kit (Vector Laboratories, Burlingame, CA) and all steps were carried out with gentle agitation on a flatbed orbital shaker. Primary polyclonal antibodies against NRAP [2] and connexin-43 (Sigma-Aldrich) were diluted 1:1000 and 1:200, respectively. Primary monoclonal antibodies against c-Myc (Clontech, clone 9E10), N-cadherin (Research Diagnostics, Flanders, NJ, RDI-NCADHERabm; or Abcam, clone GC-4) and vinculin (Sigma-Aldrich, clone VIN-11-5) were diluted 1:200, and antibody against sarcomeric α-actinin (Sigma-Aldrich, clone Ea-53) was diluted 1:1000. Polyclonal and monoclonal primary antibodies were detected with Alexa fluor 568-linked goat anti-rabbit and Alexa fluor 488-linked goat anti-mouse secondary antibodies (Invitrogen) diluted 1:1000. Immunofluorescence experiments were not optimized to yield quantitative information; therefore relative levels of detected proteins cannot be inferred from staining intensities [21].

Fluorescent images were captured using a Zeiss Axiovert 135 inverted microscope equipped with a Photometrics CoolSNAP fx CCD camera (Roper Scientific, Tuscon, AZ) and interfaced with a Macintosh computer running iVision software (BioVision Technologies, Exton, PA), as previously described [20]. Fluorescent images were background-subtracted with ImageJ, a variant of the NIH Image software program developed at the U.S. National Institutes of Health and available on the internet at http://rsb.info.nih.gov/nih-image/. The widths of cardiomyocytes that were longitudinally oriented were measured in micrographs of sections stained with antibodies against vinculin that were captured using a 40X objective.

In Vivo Echocardiography

Echocardiography data was collected and analyzed by an investigator blinded to genotype. Animals were lightly anesthetized and maintained with isoflurane anesthesia and kept warm using a heated stage and radiant heat lamp. Echocardiography was performed using a Vevo 770 High-Resolution In Vivo Imaging System (VisualSonics, Toronto, ON, Canada) with a RMV 707 “high frame” scan head at a center frequency of 30 MHz and a frequency band of 15–45 MHz, as previously described [22]. Warmed coupling gel was applied between the skin and scan head. Transverse images at the papillary muscle level were collected in B-mode and M-mode, and left ventricular wall thicknesses and chamber diameter were averaged from measurements taken in M-mode over three cardiac cycles.

In Vivo Magnetic Resonance Imaging

MRI (magnetic resonance imaging) data was collected and analyzed by an investigator blinded to genotype. Experiments were performed in a 7.0T, 16-cm horizontal Bruker MR imaging system (Bruker, Billerica, MA) with Bruker ParaVision 4.0 software. Mice were anesthetized with 1.5-3.0% isoflurane and imaged with ECG and respiratory detection (SA Instruments, Stony Brook, NY) and temperature detection (FISO fiber optics, Quebec, Canada) using a 38 mm Bruker birdcage volume coil. Magnevist (Bayer HealthCare, Montville, NJ) diluted 1:10 with sterile 0.9% saline, was administered intravenously at 0.3 mmol Gd /kg. T1 weighted gradient echo cine images of the heart were acquired in short axis from base to apex (6 slices) with the following parameters: repetition time TR = 10 to 12 ms, echo time TE= 3.4 ms, 10 to 13 frames, 30 degree flip angle, 3-4 averages, 1.0 mm slice thickness, 2.8 to 3.0 cm field of view, 256×256 matrix, respiratory and ECG-gated. Cardiac MRI data was processed to determine ejection fractions, ventricular volumes and associated functional parameters using CAAS-MRV-FARM software (Pie Medical Imaging, Netherlands.)

Data Analysis

Statistical analysis was performed on a Macintosh computer using Kaleidagraph software (Synergy Software, Reading, PA). Results are reported as means ± s.e.m. One way analysis of variance was used to test for differences among the 4 genotypes, and Fisher's LSD was used as a post-hoc test to compare all possible combinations of group pairs.

RESULTS

NRAP Overexpression

Founder mice were screened by Southern blot for the presence of the N-RAP transgene, and positive animals were mated with wild type to establish the N-RAP transgenic lines. Progeny carrying the N-RAP transgene were mated with the MHC-tTA line and all animals produced from these matings were assayed by PCR for the presence of the tTA and myc-NRAP genes (figure 1). Double transgenic animals born from these matings were tested for myc-NRAP expression by QPCR and western blot. Myc-NRAP protein expression was specifically detected in hearts of double transgenic animals, but was absent in all animals that did not carry both transgenes (figure 2A). In a screen of double transgenic animals, myc-NRAP protein was detected in the hearts of 4 of 10 independent lines (figure 2B), and in two of these lines (H1005 and H1033) total NRAP protein detected with a polyclonal anti-NRAP antibody was present at greater than two times the level found in nontransgenic controls (figures 2A and 2B). We verified that transgenic myc-NRAP expression was cardiac specific, as myc-NRAP mRNA was detected in hearts of double transgenic animals by RT-PCR, but was not detected in skeletal muscle, lung, liver, kidney, spleen, or brain (data not shown). In pilot experiments, we found that double transgenic animals exposed to doxycycline throughout embryonic development and the first three weeks after birth failed to express the transgene, even after 22 weeks following removal of the drug. In contrast, double transgenic animals never exposed to doxycycline expressed constant levels of the transgenic mRNA during this period (figure 2C). Clearly, transient exposure to doxycycline can result in chronic suppression of transgene expression in this system. Except where noted, all subsequent experiments reported were conducted using animals from line H1033 that had never been exposed to doxycycline. Hearts from these animals continued to overexpress NRAP up to at least 50 weeks of age, containing more than two times the normal level of NRAP protein found in wild type hearts (figure 2D). No increase in mortality was observed in the NRAP overexpressing animals during this study.

Immunofluorescence detection using an anti-myc primary antibody revealed significant levels of background staining even in hearts from nontransgenic controls. However, specific localization of the transgenic myc-NRAP protein was detected only in the double transgenic hearts, where myc labeling was colocalized with anti-NRAP labeling at the intercalated disks (figure 3). Similar results were observed in hearts from 10 week old and 40 week old animals.

Gross Cardiac Structure and Function

The tTA/myc-NRAP transgenic mice had normal body and heart weights, and there were no differences in heart weight/body weight ratios among the four genotypes resulting from mating the tTA-transgenic and myc-NRAP transgenic lines (data not shown). Echocardiography failed to demonstrate any large change in left ventricular wall thickness, inner diameter, or fractional shortening in the 12 week old animals (figure 4, open bars). However, left ventricular mass calculated from echocardiography data was equally elevated in both the tTA-transgenic and the tTA/myc-NRAP double transgenic animals (figure 4D, open bars), consistent with previous data on the tTA-transgenic mice [23]. At 45 weeks the left ventricle exhibited a small but significant dilation in both the tTA-transgenic and the tTA/myc-NRAP double transgenic animals, and both of these genotypes also exhibited a small decrease in mean fractional shortening (figure 4, filled bars). The tTA-transgenic hearts also exhibited a significant increase in left ventricular mass at this age.

Histological assessment was performed using transeverse sections of the heart taken from the mid-ventricular region and stained with H&E (figure 5A). No large changes were observed in left ventricular wall thicknesses or chamber diameter (figure 5B-D). However, dilation of the right ventricle was observed as an increase in that chamber's inner diameter in the NRAP-overexpressing double transgenic animals (figure 5F), while no significant change was observed in the thickness of the right ventricular free wall (figure 5E). Examination of the H&E stained cardiac sections at higher magnification did not reveal any obvious loss of cardiomyocytes or cardiac inflammation in the NRAPoverexpressing double transgenic animals (data not shown).

In order to explore right ventricular structure and function in vivo, we imaged hearts of 40-50 week old animals by MRI (figure 6). The right ventricles exhibited pronounced changes in the double transgenic NRAP-overexpressing hearts (figure 6A). The right ventricular chamber was significantly dilated in these animals (figure 6D), and ejection fraction was reduced ~40% compared to the tTA-transgenic controls and ~65% compared to the wild type controls (figure 6E). In contrast, the MRI data showed that left ventricular chamber volumes were only slightly elevated in the tTA/myc-NRAP mice, and this was accompanied by a small decrease in left ventricular ejection fraction (figure 6B,C).

Cardiomyopathy Markers and Intercalated Disks

The effect of cardiac NRAP overexpression on expression of selected cardiomyopathy markers was assessed by quantitative real-time PCR. These largely consist of genes that are highly expressed during fetal cardiac development, but that are reexpressed postnatally during cardiac hypertrophy. They include the natriuretic peptides ANP and BNP, as well as fetal isoforms of structural genes such as skeletal α-actin and ß-myosin heavy chain (MHC). All of these markers were increased in hearts from 40-50 week old tTA-transgenic and tTA/NRAP double transgenic mice compared to nontransgenic controls; in addition, mean BNP and skeletal α-actin mRNA levels were greater in the NRAP overexpressing double transgenics than in the tTA-transgenic hearts (figure 7A).

We also quantitated expression of genes encoding proteins found at the cardiac intercalated disk. N-cadherin and MLP mRNA levels did not vary between the genotypes (figure 7B). However, connexin-43 transcript levels were equally decreased in both tTAtransgenic and tTA/NRAP double transgenic mice compared to nontransgenic controls, while nonmuscle myosin heavy chain IIB transcripts were elevated (figure 7B). Immunoblot analysis demonstrated that the changes in connexin-43 and nonmuscle myosin IIB transcripts were accompanied by similar changes in protein levels (figure 7C). In addition, N-cadherin protein levels were decreased in all single and double transgenic groups relative to nontransgenic wild type hearts, but no differences were observed between the single and double transgenic groups (figure 7C). Total NRAP protein levels were specifically elevated in the double transgenic hearts from 40-50 week old animals used in these studies (figure 7C).

Immunofluorescence staining of proteins localized at cardiac intercalated disks showed no abnormalities caused by NRAP overexpression (figure 8). Intercalated disks marked by NRAP antibodies in double transgenic hearts contained the transgenic myc-NRAP protein. N-cadherin, connexin-43, and vinculin were appropriately concentrated at the intercalated disks. Sarcomeric α-actinin staining was also normal, exhibiting striated patterns in the double transgenic hearts that were indistinguishable from staining in the wild type controls (figure 8). The examples shown in figure 8 are taken from the intraventricular septum, but similar results were observed in the free walls of the right and left ventricles.

Quantitation of cell width showed that N-RAP overexpression in cardiomyocytes was associated with a ~10% hypertrophy: Mean cardiomyocyte width was 30.6 ± 0.4 μm in wild type animals, 29.4 ± 0.5 μm in tTA negative/myc-NRAP positive animals, 32.0 ± 0.4 μm in tTA positive/myc-NRAP negative animals, and 34.5 ± 0.5 μm in tTA positive/myc-NRAP positive animals; the cell width in double transgenic animals was significantly greater than in each of the other genotypes ($p < 0.001$).

DISCUSSION

NRAP Overexpression Leads to Impaired Right Ventricular Function

Echocardiography at 12 weeks revealed a modest increase in left ventricular mass in tTA-transgenic animals, with no additional change caused by NRAP overexpression and no impairment of left ventricular function (figure 4, open bars). By 40 weeks the tTAtransgenic and tTA-NRAP double transgenic animals exhibited a small dilation of the left ventricle (figure 4, filled bars). Histological analysis confirmed the absence of a large effect on left ventricular structure due to NRAP overexpression, but suggested that right ventricular function might be compromised (figure 5). MRI imaging revealed that NRAP overexpression was associated with severe dilation and impaired ejection in the right ventricles, and also confirmed the absence of a large effect on left ventricular structure and function (figure 6).

Increased expression of cardiomyopathy markers was observed in NRAP overexpressing transgenic hearts. The natriuretic peptides ANP and BNP have been used as markers for cardiomyopathy in human patients, as their expression is induced as an adaptive response to pathologic changes in the heart [24]. Similarly, hypertrophic cardiomyopathic rodents upregulate markers of an embryonic gene program that includes ANP, skeletal α-actin, and ß-MHC [25-27]. Transgenic tTA mice exhibited increased expression of ANP, BNP, skeletal actin and ß-MHC, and NRAP overexpression further elevated BNP and skeletal actin levels (figure 7A). Although plasma concentrations of ANP are elevated in dilated cardiomyopathy patients, concentrations of this peptide in cardiac tissue are unaltered; when measuring changes of natriuretic peptides in heart tissue itself, BNP appears to be a much

more sensitive marker for cardiomyopathy [28]. Therefore the large increase in BNP expression observed in NRAP-overexpressing transgenic mice along with increased skeletal α-actin supports generation of a significant cardiomyopathic response in response to excess NRAP.

Intercalated Disks in Cardiomyopathy

Cardiac intercalated disks are altered in human dilated cardiomyopathy as well as in animal models of the disease, with common features including upregulation of adherens junction proteins, including N-cadherin and NRAP, and increased convolution of the intercalated disk membrane [6,12]. These common features have led to speculation that intercalated disk defects are intrinsic to the pathophysiology of the disease [12].

We found that cardiac-specific tTA expression decreased connexin-43 and increased NMHC IIB mRNA and protein levels, but no additional changes were observed in response to overexpression of NRAP (figure 7B,C). Importantly, NRAP overexpression did not affect N-cadherin levels. In addition, immunofluorescence signals obtained with antibodies against intercalated disk proteins did not exhibit a broadening that would be indicative of increased convolution at the intercalated disk membrane (figure 8). These data indicate that the early upregulation of NRAP in MLP knockout mice and tropomodulin-overexpressing transgenic mice is unlikely to be responsible for the remodeling of the intercalated disks observed in those models [6].

Taken together, the data suggest that multiple pathophysiological pathways are activated in DCM. MLP knockout and tropomodulin-overexpression activate a pathway leading to NRAP upregulation, along with a parallel pathway leading to increased Ncadherin levels and remodeling of the intercalated disks. Previous work has shown that transgenic overexpression of N-cadherin can itself cause remodeling of intercalated disks leading to DCM [29], while the present results show that NRAP upregulation itself does not lead to significant left ventricular DCM. Instead, NRAP upregulation causes significant right ventricular dysfunction, although the mechanisms involved are unknown. However, mutations in desmosomal junction proteins of the intercalated disk have been linked to arrhythmogenic right ventricular cardiomyopathy, a disease characterized by right ventricular dilation and decreased ejection fraction with little impairment of left ventricular function [30-32]. Additional hallmarks of this disease include electrophysiological defects beginning in the early stages and fibrofatty replacement of myocardium in the late stages. Further characterization will be needed to determine if NRAP overexpression leads to these other features of arrhythmogenic right ventricular cardiomyopathy.

The Cardiac-Specific Tet-off System: Complications and Cautions

Previous studies have documented that tTA expression in the heart can cause cardiomyopathy, and that the original cardiac-specific tTA-expressing strain developed by Fishman and colleagues and used here exhibits a mild dilated cardiomyopathy [23,33]. Our results confirm this, and extend the findings to older animals than previously described; by 12 weeks, mice expressing tTA in the heart exhibited increased left ventricular mass, and by 40 weeks mild dilation was observed (figure 4). These effects were accompanied by increased expression of natriuretic factors, skeletal α-actin, and ß-MHC, along with reduced expression of connexin-43, indicating a significant cardiomyopathic response (figure 7). As emphasized by previous investigators [23], carefully designed studies with appropriate controls are essential to avoid misinterpreting data from bi-transgenic systems; our analysis of all four genotypes derived from mating hemizygous tTA-transgenic mice with hemizygous myc-NRAP transgenic mice allowed us to unambiguously identify effects of NRAP overexpression.

In pilot experiments, we found that double-transgenic animals exposed to doxycycline in utero and for the first three weeks after birth exhibited essentially irreversible inhibition of myc-NRAP transgene expression (figure 2C). Previous investigators documented that doxycycline is cleared from mice much more slowly than tetracycline [34], but to our knowledge a complete irreversibility of doxycycline-induced inhibition after withdrawing the drug for five months has not been previously reported. In addition, we found that the tTA-transgenic hemizygous males resulting from a strain rederived from frozen embryos obtained from the Jackson Laboratories were infertile. Infertility in previously described strains and irreversible inhibition by doxycycline are two possibilities to carefully consider when difficulties arise in the development of new strains for use in tetracycline-sensitive binary genetic systems.

Acknowledgments

This research was supported by the Intramural Research Program of the National Institute of Arthritis and Musculoskeletal and Skin Diseases of the National Institutes of Health. We thank Dr. Lionel Feigenbaum (Laboratory Animal Sciences Program of the National Cancer Institute, Frederick, MD) for producing the transgenic myc-NRAP founder mice, and Dr. Kimberly Makar (NIAMS) for assistance with the design of the myc-NRAP transgene. We are grateful to Dr. Brenda Klaunberg (NIH Mouse Imaging Facility) for facilitating this work, and to Dr. Klaunberg and Dr. Bob Adelstein (NHLBI) for helpful comments on the manuscript.

Abbreviations

ANP	atrial natriuretic peptide
BNP	brain natriuretic peptide
DCM	dilated cardiomyopathy
dox	doxycycline
H&E	hematoxylin and eosin
MHC	myosin heavy chain
MLP	muscle LIM protein
MRI	magnetic resonance imaging
NMHCIIB	nonmuscle myosin heavy chain IIB
TOT	tropomodulin-overexpressing transgenic
tTA	tetracycline-controlled transactivator

REFERENCES

1. Severs NJ. The cardiac muscle cell. Bioessays. 2000; 22:188–199. [PubMed: 10655038]
2. Luo G, Zhang JQ, Nguyen TP, Herrera AH, Paterson B, Horowits R. Complete cDNA sequence and tissue localization of N-RAP, a novel nebulin-related protein of striated muscle. Cell Motil Cytoskeleton. 1997; 38:75–90. [PubMed: 9295142]
3. Herrera AH, Elzey B, Law DJ, Horowits R. Terminal regions of mouse nebulin: sequence analysis and complementary localization with N-RAP. Cell Motil Cytoskeleton. 2000; 45:211–222. [PubMed: 10706776]
4. Zhang JQ, Elzey B, Williams G, Lu S, Law DJ, Horowits R. Ultrastructural and biochemical localization of N-RAP at the interface between myofibrils and intercalated disks in the mouse heart. Biochemistry. 2001; 40:14898–14906. [PubMed: 11732910]
5. Lu S, Carroll SL, Herrera AH, Ozanne B, Horowits R. New N-RAP-binding partners α-actinin, filamin and Krp1 detected by yeast two-hybrid screening: implications for myofibril assembly. J Cell Sci. 2003; 116:2169–2178. [PubMed: 12692149]

6. Ehler E, Horowits R, Zuppinger C, Price RL, Perriard E, Leu M, Caroni P, Sussman M, Eppenberger HM, Perriard JC. Alterations at the intercalated disk associated with the absence of muscle LIM protein. J Cell Biol. 2001; 153:763–772. [PubMed: 11352937]
7. Luo G, Herrera AH, Horowits R. Molecular interactions of N-RAP, a nebulin-related protein of striated muscle myotendon junctions and intercalated disks. Biochemistry. 1999; 38:6135–6143. [PubMed: 10320340]
8. Manisastry SM, Zaal KJ, Horowits R. Myofibril assembly visualized by imaging N-RAP, alpha-actinin, and actin in living cardiomyocytes. Exp Cell Res. 2009; 315:2126–2139. [PubMed: 19233165]
9. Dhume A, Lu S, Horowits R. Targeted disruption of N-RAP gene function by RNA interference: A role for N-RAP in myofibril organization. Cell Motil Cytoskeleton. 2006; 63:493–511. [PubMed: 16767749]
10. Carroll S, Lu S, Herrera AH, Horowits R. N-RAP scaffolds I-Z-I assembly during myofibrillogenesis in cultured chick cardiomyocytes. J Cell Sci. 2004; 117:105–114. [PubMed: 14657273]
11. Hall DG, Morley GE, Vaidya D, Ard M, Kimball TR, Witt SA, Colbert MC. Early onset heart failure in transgenic mice with dilated cardiomyopathy. Pediatr Res. 2000; 48:36–42. [PubMed: 10879798]
12. Perriard JC, Hirschy A, Ehler E. Dilated cardiomyopathy: a disease of the intercalated disc? Trends Cardiovasc Med. 2003; 13:30–38. [PubMed: 12554098]
13. Elliott P. Cardiomyopathy. Diagnosis and management of dilated cardiomyopathy. Heart. 2000; 84:106–112. [PubMed: 10862601]
14. Schonberger J, Seidman CE. Many roads lead to a broken heart: the genetics of dilated cardiomyopathy. Am J Hum Genet. 2001; 69:249–260. [PubMed: 11443548]
15. Chien KR. Stress pathways and heart failure. Cell. 1999; 98:555–558. [PubMed: 10490095]
16. Arber S, Hunter JJ, Ross J Jr. Hongo M, Sansig G, Borg J, Perriard JC, Chien KR, Caroni P. MLP-deficient mice exhibit a disruption of cardiac cytoarchitectural organization, dilated cardiomyopathy, and heart failure. Cell. 1997; 88:393–403. [PubMed: 9039266]
17. Sussman MA, Welch S, Cambon N, Klevitsky R, Hewett TE, Price R, Witt SA, Kimball TR. Myofibril degeneration caused by tropomodulin overexpression leads to dilated cardiomyopathy in juvenile mice. J Clin Invest. 1998; 101:51–61. [PubMed: 9421465]
18. Gehmlich K, Geier C, Osterziel KJ, Van Der Ven PF, Furst DO. Decreased interactions of mutant muscle LIM protein (MLP) with N-RAP and alpha-actinin and their implication for hypertrophic cardiomyopathy. Cell Tissue Res. 2004; 317:129–136. [PubMed: 15205937]
19. Yu Z, Redfern CS, Fishman GI. Conditional transgene expression in the heart. Circ Res. 1996; 79:691–697. [PubMed: 8831492]
20. Lu S, Borst DE, Horowits R. N-RAP expression during mouse heart development. Dev Dyn. 2005; 233:201–212. [PubMed: 15765519]
21. Basgen JM, Nevins TE, Michael AF. Quantitation of antigen in tissue by immunofluorescence image analysis. J Immunol Methods. 1989; 124:77–83. [PubMed: 2478638]
22. Isenberg JS, Qin Y, Maxhimer JB, Sipes JM, Despres D, Schnermann J, Frazier WA, Roberts DD. Thrombospondin-1 and CD47 regulate blood pressure and cardiac responses to vasoactive stress. Matrix Biol. 2009; 28:110–119. [PubMed: 19284971]
23. McCloskey DT, Turnbull L, Swigart PM, Zambon AC, Turcato S, Joho S, Grossman W, Conklin BR, Simpson PC, Baker AJ. Cardiac transgenesis with the tetracycline transactivator changes myocardial function and gene expression. Physiol Genomics. 2005; 22:118–126. [PubMed: 15797971]
24. Gardner DG. Natriuretic peptides: markers or modulators of cardiac hypertrophy? Trends Endocrinol Metab. 2003; 14:411–416. [PubMed: 14580760]
25. Freeman K, Colon-Rivera C, Olsson MC, Moore RL, Weinberger HD, Grupp IL, Vikstrom KL, Iaccarino G, Koch WJ, Leinwand LA. Progression from hypertrophic to dilated cardiomyopathy in mice that express a mutant myosin transgene. Am J Physiol Heart Circ Physiol. 2001; 280:H151–159. [PubMed: 11123229]

26. Boluyt MO, O'Neill L, Meredith AL, Bing OH, Brooks WW, Conrad CH, Crow MT, Lakatta EG. Alterations in cardiac gene expression during the transition from stable hypertrophy to heart failure. Marked upregulation of genes encoding extracellular matrix components. Circ Res. 1994; 75:23–32. [PubMed: 8013079]
27. Jones WK, Grupp IL, Doetschman T, Grupp G, Osinska H, Hewett TE, Boivin G, Gulick J, Ng WA, Robbins J. Ablation of the murine alpha myosin heavy chain gene leads to dosage effects and functional deficits in the heart. J Clin Invest. 1996; 98:1906–1917. [PubMed: 8878443]
28. Wei CM, Heublein DM, Perrella MA, Lerman A, Rodeheffer RJ, McGregor CG, Edwards WD, Schaff HV, Burnett JC Jr. Natriuretic peptide system in human heart failure. Circulation. 1993; 88:1004–1009. [PubMed: 8353861]
29. Ferreira-Cornwell MC, Luo Y, Narula N, Lenox JM, Lieberman M, Radice GL. Remodeling the intercalated disc leads to cardiomyopathy in mice misexpressing cadherins in the heart. J Cell Sci. 2002; 115:1623–1634. [PubMed: 11950881]
30. Basso C, Corrado D, Marcus FI, Nava A, Thiene G. Arrhythmogenic right ventricular cardiomyopathy. Lancet. 2009; 373:1289–1300. [PubMed: 19362677]
31. Tsatsopoulou AA, Protonotarios NI, McKenna WJ. Arrhythmogenic right ventricular dysplasia, a cell adhesion cardiomyopathy: insights into disease pathogenesis from preliminary genotype--phenotype assessment. Heart. 2006; 92:1720–1723. [PubMed: 16698823]
32. Sen-Chowdhry S, Syrris P, McKenna WJ. Genetics of right ventricular cardiomyopathy. J Cardiovasc Electrophysiol. 2005; 16:927–935. [PubMed: 16101641]
33. Sanbe A, Gulick J, Hanks MC, Liang Q, Osinska H, Robbins J. Reengineering inducible cardiac-specific transgenesis with an attenuated myosin heavy chain promoter. Circ Res. 2003; 92:609–616. [PubMed: 12623879]
34. Robertson A, Perea J, Tolmachova T, Thomas PK, Huxley C. Effects of mouse strain, position of integration and tetracycline analogue on the tetracycline conditional system in transgenic mice. Gene. 2002; 282:65–74. [PubMed: 11814678]
35. Guo HG, Sadowska M, Reid W, Tschachler E, Hayward G, Reitz M. Kaposi's sarcoma-like tumors in a human herpesvirus 8 ORF74 transgenic mouse. J Virol. 2003; 77:2631–2639. [PubMed: 12552002]
36. Tsujita Y, Muraski J, Shiraishi I, Kato T, Kajstura J, Anversa P, Sussman MA. Nuclear targeting of Akt antagonizes aspects of cardiomyocyte hypertrophy. Proc Natl Acad Sci U S A. 2006; 103:11946–11951. [PubMed: 16882732]
37. Karabekian Z, Gillum ND, Wong EW, Sarvazyan N. Effects of N-cadherin overexpression on the adhesion properties of embryonic stem cells. Cell Adh Migr. 2009; 3:305–310. [PubMed: 19377287]
38. Cerutti C, Kurdi M, Bricca G, Hodroj W, Paultre C, Randon J, Gustin MP. Transcriptional alterations in the left ventricle of three hypertensive rat models. Physiol Genomics. 2006; 27:295–308. [PubMed: 16882881]

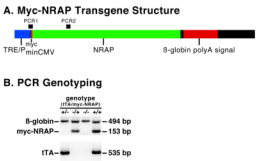

Figure 1.

(A) Schematic diagram of the myc-NRAP transgene. A tet response element (TRE) and minimal CMV promoter (P_{minCMV}) combine to form the promoter region. A myc epitope tag is fused in frame to the NRAP coding sequence. Also shown are the locations of PCR products amplified from the myc-NRAP transgene or its mRNA (PCR1) or total NRAP mRNA (endogenous plus transgenic) (PCR2). (B) Genotyping by PCR analysis of genomic DNA. Amplification of a 153 bp product encoding the myc epitope region of the transgene (PCR1 in A above) indicates an animal carries the myc-NRAP transgene. A 535 bp product was specifically amplified from animals carrying the tTA transgene using previously described primers. A 494 bp product amplified from the ß-globin gene served as a positive control. Crossing tTA hemizygotes with myc-NRAP hemizygotes typically yielded each of the four possible combinations of genotypes in approximately equal proportion. In this and subsequent figures, the four genotypes are indicated by a plus or minus to indicate the presence or absence of each transgene, with the presence or absence of the tTA and myc-NRAP transgenes given by the first and second symbol, respectively.

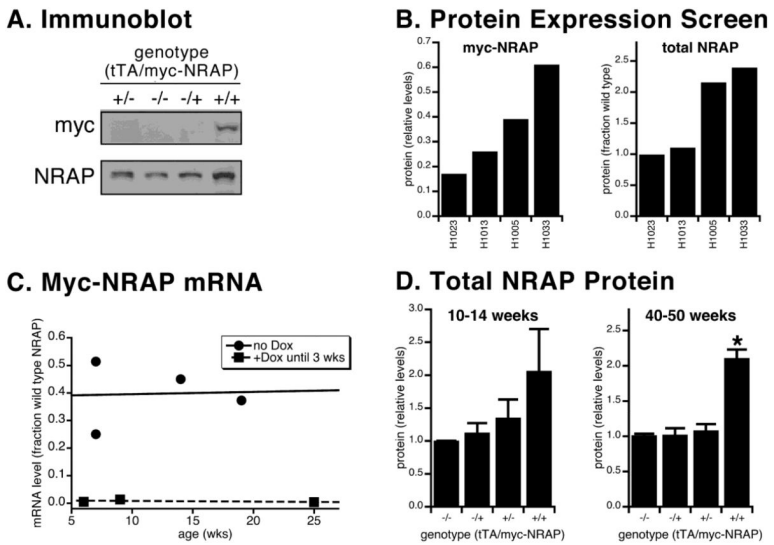

Figure 2.

(A) Immunoblot detection of the myc-NRAP transgenic protein and total NRAP in hearts from animals born by crossing tTA transgenic females with myc-NRAP transgenic males. (B) myc-NRAP protein and total NRAP measured by quantitation of immunoblots of hearts from 5-10 week old double transgenic animals from independent lines. The H1005 and H1033 lines contain more than two times the level of total cardiac NRAP found in wild type controls. (C) myc-NRAP mRNA levels detected by real time RT-PCR in double transgenic animals from line H1023. Exposure to doxycycline from conception to the first three weeks after birth prevented expression of myc-NRAP up to at least 25 weeks of age. (D) Total NRAP protein of line H1033 animals at 10-14 weeks and 40-50 weeks. Increased cardiac NRAP expression in double transgenic animals persists in this line throughout the time period studied. In (A) and (D), the four genotypes are indicated by a plus or minus to indicate the presence or absence of each transgene, with the presence or absence of the tTA and myc-NRAP transgenes given by the first and second symbol, respectively. Bars in D represent the mean ± s.e.m. from 3-12 animals. *significantly different from all other genotypes ($p < 0.05$).

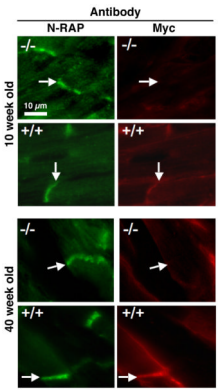

Figure 3.

(A) Double immunofluorescence staining for total NRAP (left panels) and myc-NRAP (right panels) in cardiac sections from 10 week and 40 week old animals from line H1005. NRAP is concentrated at the intercalated disks in wild type (−/−) and double transgenic (+/+) animals (arrows, left panels). These same structures are detected by anti-myc antibodies in the double transgenic hearts, while intercalated disks in wild type animals remain unstained (arrows, right panels).

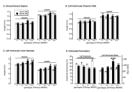

Figure 4.

Echocardiography data from 10-14 week (open bars) and 40-50 week (filled bars) animals. The four genotypes are indicated by a plus or minus to indicate the presence or absence of each transgene, with the presence or absence of the tTA and myc-NRAP transgenes given by the first and second symbol, respectively. *significantly different from −/− and −/+ ($p < 0.05$). **significantly different from −/− ($p < 0.01$). ***significantly different from all other genotypes ($p < 0.05$). Each open or closed bar represents the mean ± s.e.m. from 4-10 animals or 8-17 animals, respectively.

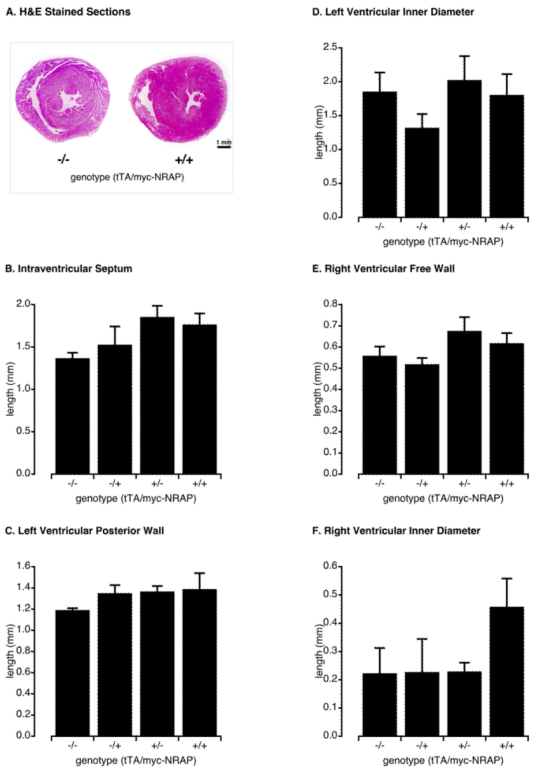

Figure 5.

Histological analysis of gross cardiac structure from 40-50 week old animals. (A) Typical transverse sections from the mid-ventricular region of wild type (−/−) and double transgenic (+/+) hearts stained with H&E. (B-F) Mean parameters for all genotypes. The four genotypes are indicated by a plus or minus to indicate the presence or absence of each transgene, with the presence or absence of the tTA and myc-NRAP transgenes given by the first and second symbol, respectively. Each bar represents the mean ± s.e.m. from 2-5 animals.

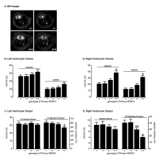

Figure 6.

Cardiac MRI from 40-50 week old animals. (A) Typical MRI images from wild type (−/−) and double transgenic (+/+) animals at end of diastole (left panels) and systole (right panels). (B-E) Mean chamber volumes and output parameters for the left ventricles (B, C) and right ventricles (D, E) for all genotypes. The four genotypes are indicated by a plus or minus to indicate the presence or absence of each transgene, with the presence or absence of the tTA and myc-NRAP transgenes given by the first and second symbol, respectively. Each bar represents the mean ± s.e.m. from 7-10 animals. (C) *significantly different from −/− and −/+ ($p < 0.05$). (D) *significantly different from all other genotypes ($p < 0.01$). (E) *significantly different from all other genotypes ($p < 0.05$). **significantly different from −/+ and +/+ ($p < 0.05$).

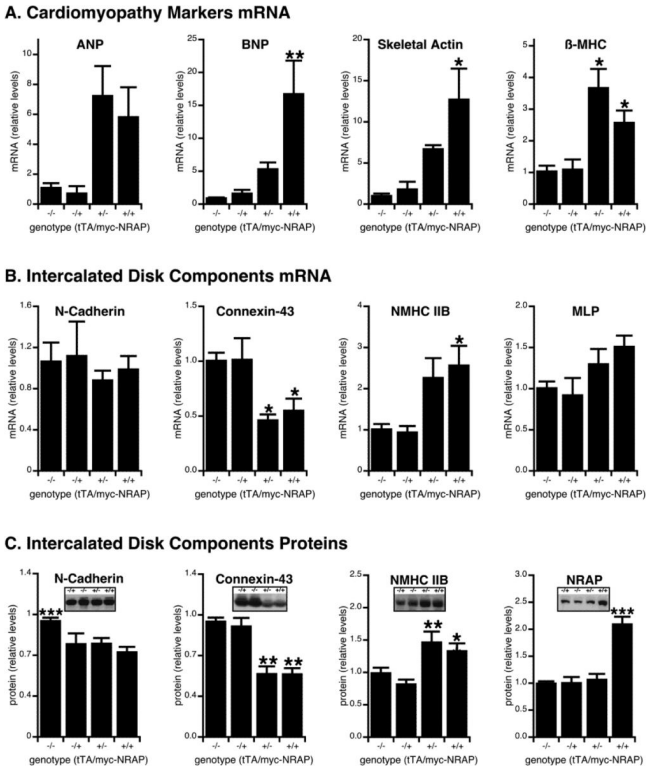

Figure 7.

Cardiac gene expression analysis from 40-50 week old animals. (A) mRNA levels of cardiomyopathy markers. *significantly different from −/− and −/+ ($p < 0.05$); **significantly different from all other genotypes ($p < 0.02$). (B) mRNA levels of intercalated disk components. *significantly different from −/− and −/+ ($p < 0.05$); (C) Protein levels of intercalated disk components. Insets show typical sample blots. *significantly different from −/+ ($p < 0.05$); **significantly different from −/− and −/+ ($p < 0.05$); ***significantly different from all other genotypes ($p < 0.05$). In all panels, the four genotypes are indicated by a plus or minus to indicate the presence or absence of each transgene, with the presence or absence of the tTA and myc-NRAP transgenes given by the first and second symbol, respectively. Each bar represents the mean ± s.e.m. from 4-12 animals.

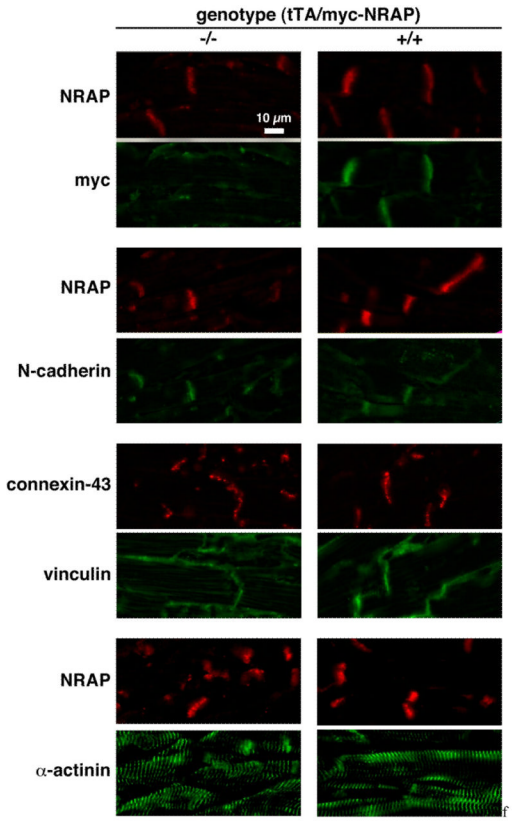

Figure 8.

Immunofluorescence localization of intercalated disk and myofibril components in 40-50 week old animals. Sections of wild type (left panels) and double transgenic (right panels) hearts were double stained with antibodies against NRAP and myc, NRAP and N-cadherin, connexin-43 and vinculin, or N-RAP and sarcomeric α-actinin, as indicated. Regions from the interventricular septum are shown.

Table 1

PCR Primer Pairs

Amplified Gene or mRNA	Primer Pair	Product Size
myc-NRAP	Forward: 5′-CTCCATAGAAGACACCGGGACCG-3′ Reverse: 5′-GCACATTCATAAACGCGTCAGTGG-3′	153 bp
tTA	Forward: 5′-TCAGACCGAGATTTCTTCCATCCC-3′ Reverse: 5′-GAATTCAGGCTCGCCTGCAGTTGG-3′	535 bp
ß-globin	Forward: 5′-CCAATCTGCTCACACAGGATAGAGAGGGCAGG-3′ Reverse: 5′-CCTTGAGGCTGTCCAAGTGATTCAGGCCATCG-3′	494 bp
total NRAP	Forward: 5′-TGCTCCACGCTCTCAAAGTTGG-3′ Reverse: 5′-TGACATCCTTCAGGGGAACCAG-3′	147 bp
ANP	Forward: 5′-GAGTGGACTAGGCTGCAACAG-3′ Reverse: 5′-GCTCCAGGAGGGTGTTCACCA-3′	163 bp
BNP	Forward: 5′-AAGTCCTAGCCAGTCTCCAGA-3′ Reverse: 5′-GAGCTGTCTCTGGGCCATTTC-3′	91 bp
skeletal α-actin	Forward: 5′-AGACCACCGCTCTTGTGTGTG-3′ Reverse: 5′-CTGACCCATACCTACCATGACACC-3′	235 bp
ß-MHC	Forward: 5′-ATGTGCCGGACCTTGGAAG-3′ Reverse: 5′-CCTCGGGTTAGCTGAGAGATCA-3′	170 bp
N-cadherin	Forward: 5′-AGGGTGGACGTCATTGTAGC-3′ Reverse: 5′- CTGTTGGGGTCTGTCAGGAT-3′	134 bp
connexin-43	Forward: 5′-GAACACGGCAAGGTGAAGAT-3′ Reverse: 5′-GACGTGAGAGGAAGCAGTCC-3′	187 bp
NMHC IIB	Forward: 5′-TGTCATCTACAACCCTGCCACTC-3′ Reverse: 5′-GCTTTCTTCCCATTCTCTGCCAG-3′	150 bp
MLP	Forward: 5′-AATCAGAGAAGTGCCCACGATG-3′ Reverse: 5′-TGCTGTGTAAGCCCTCCAAACC-3′	220 bp

PCR primers used to amplify the indicated products. The primers for tTA [19], ß-globin [35], total NRAP, MLP, and NMHCIIB [9], BNP, skeletal α-actin, and ß-MHC [36], and N-cadherin and connexin-43 [37] have been described previously. The primers for ANP are based on those previously described for rat [38].